Spin-Peierls ground states in an electron-lattice periodic Anderson model

1999 J. Phys.: Condens. Matter 11 3547

(http://iopscience.iop.org/0953-8984/11/17/312)

J. Phys.: Condens. Matter **11** (1999) 3547–3554. Printed in the UK PII: S0953-8984(99)00905-4

Spin–Peierls ground states in an electron–lattice periodic Anderson model

Ya-Sha Yi, A R Bishop and H Röder

Theoretical Division and Center for Nonlinear Studies, Los Alamos National Laboratory, Los Alamos, NM 87545, USA

Received 12 January 1999

Abstract. Novel dimerized antiferromagnetic (homogeneous spin–Peierls) and inhomogeneous-lattice antiferromagnetic (inhomogeneous spin–Peierls) ground states are found in a one-dimensional (1-D) and a two-dimensional (2-D) electron–lattice periodic Anderson model, respectively. Coexistence and mutual enhancement of the Peierls lattice distortion and the antiferromagnetic long-range-order are emphasized. The stoichiometric (half-filling) phase diagrams for the 1-D and 2-D cases are strongly dependent on the hybridization and electron–lattice coupling. For non-stoichiometric fillings, local lattice distortion (coupled spin–charge–lattice small-polaron) states are found: these are discussed in the context of, for example, Ce-based, heavy-fermion systems. Relations to volume collapse phenomena and inorganic spin–Peierls systems, and the similarity of the phase diagrams to those of organic superconductors are also described.

The periodic Anderson model (PAM) has attracted intensive theoretical study as a minimal model for describing many phenomena observed in rare-earth and actinide materials [1–5], especially heavy-fermion systems such as Ce and U compounds. The competition between RKKY and Kondo interactions, volume collapse phenomena under pressure [6–10], the spin (charge) gap, and the rich broken-symmetry phases in these materials are widely studied within the framework of the PAM. However, lattice effects in these systems have also been implicated in several experiments [11, 12]. The pressure-induced volume collapse and the doping with other rare-earth elements, which leads to a phase transition between antiferromagnetic and spin-liquid states, are each accompanied by a unit-cell volume change. There are also strong magnetoelastic effects, especially in superconducting heavy-fermion compounds. These observations strongly indicate the importance of lattice effects and electron–lattice coupling. Recently, evidence for a local lattice distortion has been found from neutron scattering in Ce-based compounds, which may suggest the existence of a polaron [13]. This is also consistent with extensive Fermi surface (e.g., photoemission [14]) evidence for flat-band regions.

To approach these qualitatively distinct effects, we here extend the PAM to include electron–lattice coupling. Explicitly, we incorporate modification of the hopping in the conduction band induced by lattice distortion. We find that, in addition to the RKKY and Kondo interactions [5], a Peierls instability strongly competes, and the competition among these three mechanisms leads to new novel broken-symmetry ground states. The phase diagrams that we find for both 1-D and 2-D cases suggest that feedback effects induced by the three coupled mechanisms can be exploited to understand several classes of complex electronic materials including spin–Peierls materials [15–17] and organic charge-transfer compounds [18, 19]. Furthermore, upon doping, we find a small-polaron state, especially near phase boundaries,

0953-8984/99/173547+08$19.50

again emphasizing the fundamental importance of the electron–lattice (e–l) coupling in these materials.

Our electron–lattice PAM (e–l PAM) Hamiltonian on a square lattice (the 1-D case can be trivially extracted from the 2-D model) is

$$\begin{aligned} H = &-t\sum_{i,\sigma}\{[1-\alpha(u^x_{i+x}-u^x_i)](d^\dagger_{i+x,\sigma}d_{i,\sigma}+\text{h.c.})+[1-\alpha(u^y_{i+y}-u^y_i)](d^\dagger_{i+y,\sigma}d_{i,\sigma}+\text{h.c.})\} \\ &+\epsilon_d\sum_{i,\sigma}d^\dagger_{i,\sigma}d_{i,\sigma}+\left(\epsilon_f-\frac{1}{2}U_f\right)\sum_{i,\sigma}f^\dagger_{i,\sigma}f_{i,\sigma} \\ &-V\sum_{i,\sigma}(d^\dagger_{i,\sigma}f_{i,\sigma}+f^\dagger_{i,\sigma}d_{i,\sigma})+U_f\sum_i f^\dagger_{i,\uparrow}f_{i,\uparrow}f^\dagger_{i,\downarrow}f_{i,\downarrow} \\ &+\frac{1}{2}K\sum_i(u^x_{i+x}-u^x_i)^2+\frac{1}{2}K\sum_i(u^y_{i+y}-u^y_i)^2+\frac{1}{2M}\sum_l P_l^2. \end{aligned} \tag{1}$$

Here t is the hopping between the neighbouring sites in the conduction d band, U_f is the on-site Coulomb interaction in the insulating f band, V is the hybridization between d and f bands, ϵ_d and ϵ_f are the site energy levels of the d and f bands. α is an electron–lattice coupling constant in the d band, $u^{x(y)}$ is the lattice displacement, K is the spring constant, and P_l is the ionic momentum. We use the following representative parameters: $t = 1$, $U_f = 4t$, $K = 20t$ Å^{-2}, and consider the symmetric case ($\epsilon_d = \epsilon_f = 0$). To accommodate the inhomogeneous and non-linear features anticipated, we use inhomogeneous self-consistent-field methods for the e–l PAM models [20]; this is a qualitative improvement on homogeneous or similar periodic methods. To determine the character of the ground state and phase diagrams, we measure the magnetization m^f_i and lattice distortion $u^{x(y)}_i$ at every site within this inhomogeneous approach. We emphasize the importance of retaining the full two-band (d, f) model to obtain the new phases described below: self-doping between the bands is essential in determining effective intersite and interorbital coupling (cf. binary-atom unit-cell cases [20]). If the ground state is homogeneous, it is also naturally obtained in our approach. Of course, the mean-field state artificially breaks symmetries and the ordered states are more advantageous within this mean-field approximation; especially in 1-D case, also, our model has a band of acoustic modes at zero energy, which enhances the tendency of the model towards symmetry breaking, but the unrestricted (inhomogeneous) implementation is a qualitative improvement on homogeneous mean-field or similar periodic methods. For the 2-D e–l PAM, our results are qualitatively the same as the quantum Monte Carlo results along the $\alpha = 0$ line [5]. When the electron–lattice interaction is becoming more important, we also expect that the inhomogeneous self-consistent-field method will capture the essential physics in the 1-D case [20]. Periodic boundary conditions are used.

In both the 1-D and 2-D cases, we find the coexistence of a long-range antiferromagnetic (AF) phase and a Peierls phase ('spin–Peierls'). Importantly, they are found to enhance each other (i.e. there is a positive feedback), instead of being destructive as in recently found inorganic spin–Peierls materials such as $CuGeO_3$ [21,22]. Depending on the hybridization V between the d and f bands and the e–l coupling constant α, various broken-symmetry phases and phase transitions are found. Upon doping away from stoichiometric filling, we also find local (polaronic) distortion states, especially near the phase boundaries, which suggests that the competition among the Peierls instability and the Kondo and RKKY interactions is vital for understanding the rich phenomena exhibited by rare-earth transition metal and related materials.

The 1-D phase diagram is shown in figure 1. Four phases are designated: spin–Peierls-I ($|m^f_i| \neq 0$ and $\langle m^f_i m^f_j\rangle \neq 0$ at large $|i-j|$, $u_i = -u_{i+1} \neq 0$; dimerization and AF

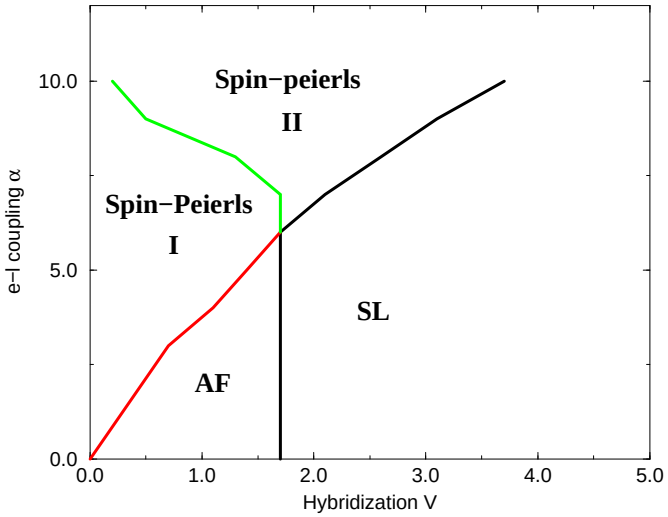

Figure 1. The 1-D phase diagram. Spin–Peierls-I and spin–Peierls-II represent the homogeneous and inhomogeneous spin–Peierls phases, respectively. AF represents the antiferromagnetic phase and SL represents the spin-liquid phase.

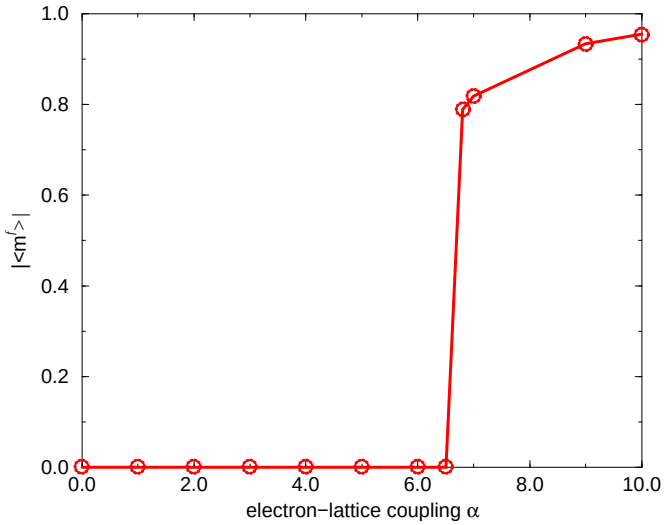

Figure 2. The variation of the magnetic moment with electron–lattice coupling α. Here $V = 2.1$.

long-range order coexist); spin–Peierls-II ($|m_i^f| \neq 0$ and $\langle m_i^f m_j^f \rangle \neq 0$ at large $|i-j|$, $u_i \neq 0$, inhomogeneous-lattice distortion and AF long-range order coexist); antiferromagnetic ($|m_i^f| \neq 0$ and $\langle m_i^f m_j^f \rangle \neq 0$ at large $|i-j|$, $u_i = 0$); and spin-liquid ($|m_i^f| = 0, u_i = 0$). When the e–l coupling has moderate strength, satisfying the condition $\alpha\,\delta u < U_f$, model (1) yields the homogeneous spin–Peierls ground state. When $\alpha\,\delta u > U_f$, the inhomogeneous spin–Peierls-II ground state is found. It can be concluded from figure 1 that lattice distortion and AF long-range order reinforce each other. As we clearly see from figures 2 and 3, with increase of the e–l coupling, there is a sharp increase of m_i^f (figure 2) and the spin–spin correlation (figure 3). This represents a phase transition from a spin-liquid phase to a spin–Peierls phase.

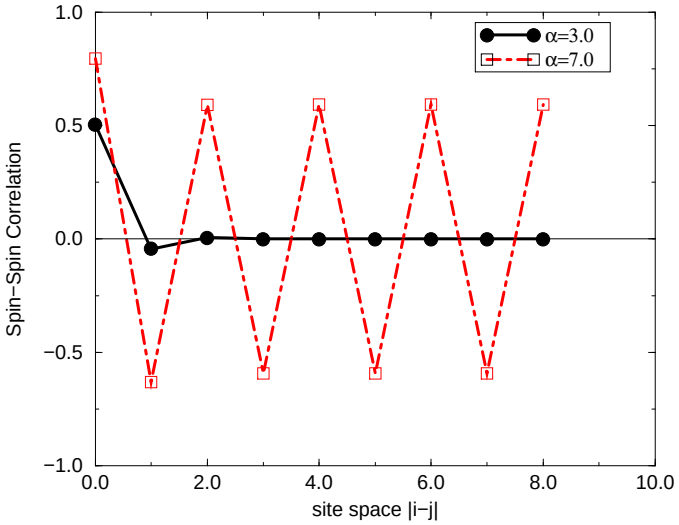

Figure 3. The spin–spin correlation $\langle m_i^f m_j^f \rangle$ in a 16-site chain, demonstrating the dependence of the long-range AF order on the e–l coupling α. Here $V = 1.9$.

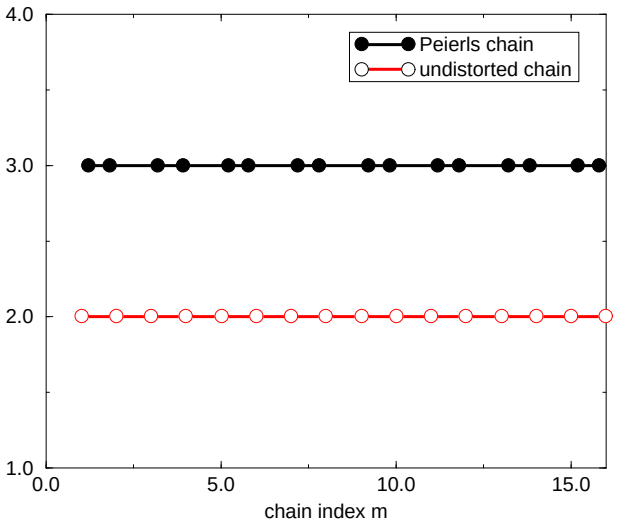

Figure 4. The dimerized spin–Peierls phase for a 16-site chain.

The corresponding dimerized lattice distortion for a 16-site chain is shown in figure 4.

A representative material value of α is $4.0t$ Å^{-1}. The effect of pressure is equivalent to changing the hybridization V between the d and f orbitals, and the e–l coupling is weakly dependent on temperature. We therefore suggest that phase transitions from spin–Peierls to AF and finally to spin-liquid phases should be observed with increasing pressure.

We have studied the 2-D case in detail for 4×4, 6×6, and 8×8 unit-cell square lattices. The phase diagram is shown in figure 5. (The 6×6 and 8×8 findings are almost quantitatively the same, so we believe that figure 5 essentially represents the large-system-size phase diagram). The general similarity of the phase diagrams in the 1-D and 2-D cases

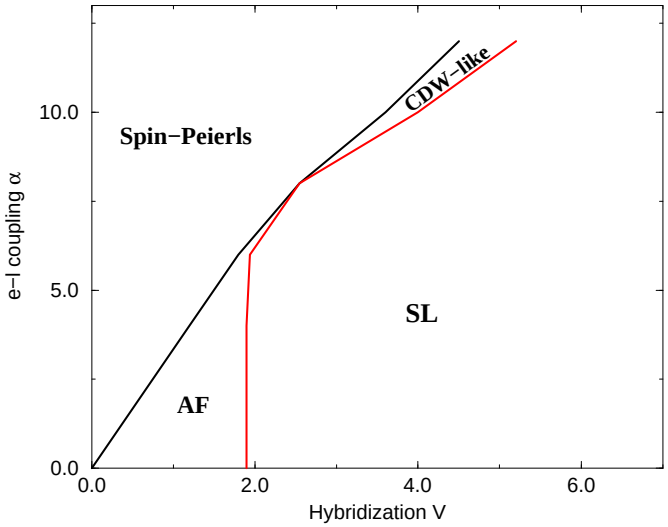

Figure 5. The phase diagram in 2-D. Note the long-period spin–Peierls ground state found in the small-V region. CDW denotes a charge-density wave.

is evident. In 2-D, the inhomogeneous spin–Peierls phase is found to be the ground state when the hybridization V and the e–l coupling α satisfy certain conditions. Unlike in the 1-D case, lattice inhomogeneity appears throughout the spin–Peierls phase. In addition to the spin–Peierls phase, the AF phase, and the spin-liquid phase, there is a new charge-density-wave-like (CDW-like) phase present in 2-D, defined by $|m_i^f| = 0$ and $u_i \neq 0$. This phase is a result of the competition between the e–l coupling and the hybridization for sufficiently strong e–l coupling. Again, in real materials with reasonable e–l coupling, phase transitions between spin–Peierls, AF, and spin-liquid phases should be observed with pressure.

We see that in both the 1-D and 2-D cases in our e–l PAM model, the striking common feature is that a new spin–Peierls ground state is found, and that there is coexistence of the Peierls distortion and AF long-range order, with positive feedback between them. The inhomogeneity of the spin–Peierls phase arises from contributions of many phonon modes, in addition to the (π, π), $(\pi, 0)$, $(0, \pi)$ modes, which drive dimerization. Since the phonon spectrum has strong dispersion, in the 2-D case the inhomogeneous spin–Peierls ground state is always found, because the contributions of other phonon modes further lower the system's energy. The 2-D lattice structure of the inhomogeneous spin–Peierls state is illustrated in figure 6 for a 4×4 system.

For low doping away from stoichiometric filling, local distortions in the form of small-polaron states are found. We find that such polaron states are most easily formed near the phase boundary between the spin–Peierls phase and the AF phase, especially near the multi-critical point separating the four phases (see figure 5). Specifically, at half-filling and in the pure AF phase but near the phase boundary, when we dope the system, a local spin–Peierls phase distortion (a composite spin–charge–lattice small polaron) is induced in the AF background. With larger doping this is a mechanism for melting and a global phase transition. This sensitivity near phase boundaries may be related to the chemical pressure phenomena, observed in many experiments [11,12]. Local distortions in a Ce-based heavy-fermion material have also recently been suggested experimentally [13]. To understand the complex rare-earth materials, and the experimentally observed phenomena, including all the spin, charge and

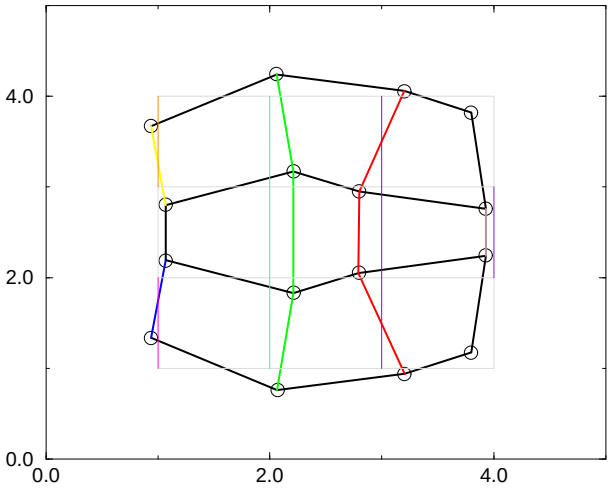

Figure 6. Typical lattice structure of the 2-D inhomogeneous spin–Peierls phase, with $\alpha = 7.0$ and $V = 1.9$

lattice effects, we believe that including cooperative spin–charge–lattice couplings and the intrinsic inhomogeneities that they drive is essential. An electron–polaron state in an AF background is illustrated in figure 7.

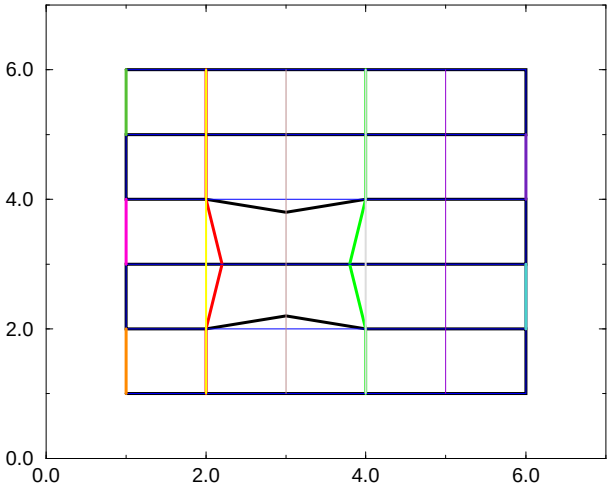

Figure 7. Local lattice distortion induced by doping away from half-filling. Here $\alpha = 4.0$ and $V = 1.6$. This polaronic lattice distortion is accompanied by localization of charge and spin, and local variation of (d, f) orbital occupation, as will be described in detail elsewhere.

The rich phase diagrams found in the e–l PAM are suggestive for several classes of complex electronic materials that exhibit interesting phenomena under pressure, temperature, and doping. For example, in organic conductors (or superconductors), the phase transition SP $\rightarrow$ AF $\rightarrow$ SDW $\rightarrow$ SL (or superconductor) with the variation of external pressure at low temperatures [23] is very similar to the phase transition of our e–l PAM model with variation of the hybridization V and appropriate e–l coupling strength. As we have noted, the application

of pressure increases the exchange between the d and f orbitals, i.e., increases V. Also, the inorganic spin–Peierls material $CuGeO_3$ shows similarities with our model's properties. When the on-site Coulomb interaction on the f orbital is very large, we can use a spin–Peierls-like model [17] to simulate our e–l PAM model. Here the AF coupling arises from the on-site f orbital electron–electron correlation, while the lattice-modified AF coupling originates from the lattice distortion between the neighbouring d orbitals (since the effective AF coupling between the neighbouring f orbitals depends on the hopping between the d orbitals (cf. [20])). Thus in this limit, the two-band e–l PAM model can be approximated with a one-band spin–Peierls-like model, which is widely exploited for both organic and inorganic spin–Peierls materials. We emphasize that we only point here to qualitative similarities between the two models. As we have shown, coexistence of the Peierls lattice distortion and the AF long-range order reinforce each other in the e–l PAM. This is significantly different from the case for the original spin–Peierls model, where these two phases are viewed as exclusive; so when doping, the dopant disorder must be included to account for the coexistence of Peierls and AF long-range order [22, 24]. The spin–Peierls ground state that we have identified in our e–l PAM model is an intrinsic feature of the two-band spin–charge–lattice coupled system.

The local distortion suggested in recent experiments on the Ce-based heavy-fermion materials [13] strongly supports the importance of the e–l interaction in these materials. Other features in our e–l PAM model concerning the magnetization, the spin–spin correlation, thermodynamics, etc, are also under investigation and will be given elsewhere, together with results for other lattice symmetries and 3-D.

In summary, we have found new homogeneous and inhomogeneous spin–Peierls ground states in an electron–lattice periodic Anderson model for both 1-D and 2-D square-lattice systems. The importance of the competition among the Peierls instability and the RKKY and Kondo interactions is evident. Lattice effects have largely been neglected in previous studies, although many experiments have strongly suggested coupled spin–charge–lattice signatures in the rare-earth materials: heavy-fermion materials exhibiting a volume collapse, and chemical pressure (doping) effects accompanied by unit-cell changes or isostructural phase transitions, especially in superconducting compounds. The small-polaron state found upon doping away from stoichiometry in our model is also in agreement with recent neutron scattering experiments [13] on the Ce materials, as well as Fermi surface structure [14]. The new ground states that we have found and the mechanism of positive feedback between the Peierls order and AF long-range order can help in the understanding of a series of materials, including inorganic spin–Peierls materials, organic conductors, and MX chain systems [20], in addition to the rare-earth compounds. In all cases, both the local polaronic distortions with doping, and the structurally inhomogeneous spin–Peierls phase will act as sources of 'intrinsic disorder' and compete with extrinsic disorder effects. This leads us to anticipate widespread evidence for metastable phases and glassy (multi-timescale) dynamics.

Acknowledgments

We have benefited from valuable discussions with A Arko, J Tinka Gammel, D Louca, R T Scalettar, and J D Thompson. This work was supported by the US Department of Energy.

References

[1] Blankenbecler R, Fulco J R, Gill W and Scalapino D J 1987 *Phys. Rev. Lett.* **58** 411
[2] Fye R M 1990 *Phys. Rev.* B **41** 2490
[3] Hirsch J E and Fye R M 1986 *Phys. Rev. Lett.* **56** 2521

[4] Silver R N, Gubernatis J E, Sivia D S and Jarrel M 1990 *Phys. Rev. Lett.* **65** 496
[5] Vekic M, Cannon J W, Scalapino D J, Scalettar R T and Sugar R L 1995 *Phys. Rev. Lett.* **74** 2367
[6] Thalmeier P 1988 *J. Magn. Magn. Mater.* **76** 299
[7] Allen J W and Martin R 1982 *Phys. Rev. Lett.* **49** 1106
[8] McMahan A K 1989 *J. Less-Common Met.* **149** 1
[9] Boring A M, Albers R C, Eriksson O and Koeling D D 1992 *Phys. Rev. Lett.* **68** 2652
[10] de Visser A, Franse J J M and Flouquet J 1989 *Physica* B **161** 324
[11] Medina A N, Hayashi M A, Cardoso L P, Gama S and Gandra F G 1998 *Phys. Rev.* B **57** 5900
[12] Movshovich R, Graf T, Mandrus D, Hundley M F, Thompson J D, Fisher R A, Philips N E and Smith J L 1996 *Physica* B **223** 126
[13] Louca D *et al*, unpublished
[14] Arko A J *et al* 1997 *Phys. Rev.* B **56** R7041
[15] Hase M, Terasaki I and Uchinokura K 1993 *Phys. Rev. Lett.* **70** 3651
[16] Bulaevskii L N, Buzdin A I and Khomskii D I 1978 *Solid State Commun.* **27** 5
[17] Uhrig G S and Schulz H J 1996 *Phys. Rev.* B **54** 9624
[18] McKenzie R H 1997 *Science* **278** 820
[19] Kino H and Fukuyama H 1996 *J. Phys. Soc. Japan* **65** 2158
[20] Yonemitsu K, Bishop A R and Lorenzana J 1993 *Phys. Rev.* B **47** 8065
Röder H, Bishop A R and Tinka Gammel J 1993 *Phys. Rev. Lett.* **70** 3498
[21] Hase M, Terasaki I, Sasago Y and Uchinokura K 1993 *Phys. Rev. Lett.* **71** 4059
[22] Fukuyama H, Tanimoto T and Saito M 1996 *J. Phys. Soc. Japan* **65** 1182
[23] Fukuyama H 1999 *Rev. High Pressure Sci. Technol.* at press
[24] Masuda T, Fujioka A, Uchiyama Y, Tsukada I and Uchinokura K 1998 *Phys. Rev. Lett.* **80** 4566